Autonomous Gripping and Carrying of Polyhedral Shaped Object based on Plane Detection by a Quadruped Tracked Mobile Robot

Toyomi Fujita and Nobuatsu Aimi
Department of Electronics and Intelligent Systems, Tohoku Institute of Technology, Sendai 982-8577, Japan

Keywords: Mobile Robot with Multiple Manipulation Arms, Autonomous Gripping, Depth Image, Plane Detection, Observation Position Computation.

Abstract: Recently, it is highly expected that robots work instead of human in a dangerous site such as disaster area. Sufficient working ability is required for such robots as well as moving ability. Thus, we present a method for autonomous gripping and carrying of a polyhedral shaped object by a mobile robot with multiple manipulation arms based on plane detection. Using this method, the robot can calculate appropriate observation positions for the detection of gripping planes and positions of the object. We apply the method to a quadruped tracked robot and verify its effectiveness in experiments for autonomous gripping and carrying of a box shaped object.

1 INTRODUCTION

In recent years, a robot is expected to perform some actions related to rescue activity in a disaster area. The robot should perform not only an exploration but also a working task by itself in the area. For such a task, the robot that has manipulation arms is useful. Therefore, we have developed several tracked mobile robots that were equipped with multiple legs which can be used as manipulation arms (Fujita and Tsuchiya, 2014) (Fujita and Tsuchiya, 2015) (Fujita and Sasaki, 2017). These robots can operate some handling tasks such as a transportation of target object using two legs by a remote control. However, it is basically difficult to control properly for such tasks.

In order to solve this problem, this study considers that such robots perform transportation tasks autonomously by detecting gripping positions of a polyhedral shaped object. Proposed method is based on the detection of gripped planes by two manipulation arms. In the method, the robot detects gripping planes and positions using a depth sensor by observing the object at several positions. We consider how to determine proper observation positions to detect them efficiently.

The following sections describe the overall method for detecting information to grip and carry a polyhedral shaped object in Section 3, how to determine the observation positions in Section 4, implemented robot system in Section 5, and experiments for proposed methods in Section 6.

2 RELATED WORKS

Recently, some autonomous planning for robot gripping have been considered.

Yamazaki et al. presented a method for object grasping by modeling based on voxel representation (Yamazaki et al., 2007). In this method, a robot observes an object from multiple views and generates a 3-D model consisting of voxel. The gripping position is determined by the area of voxel and posture of the hand. It may be difficult for our aim to apply because the robot needs to move the area surrounding object to capture multi-viewpoint images.

Masuda and Lim presented a method for plane detection utilizing 3-D Hough transform and a structure of retina (Masuda and Lim, 2014). However, gripping planning is not considered after the plane detection.

We present a method based on plane detection of a polyhedral object and obtain planes on which the robotic arms can grip and manipulate by their hands. Gu et al. presented a grip planning method to generate optimal collision-free grip sequences for a biped climbing robot based on a pole detection and grasping pose computation using depth and image data(Gu et al., 2017)(Gu et al., 2018). This method mainly considers point and line information as geometric information. This study, on the other hand, mainly consider plane information of a polyhedral object.

In the method presented by Harada et al., the shape of object was obtained as a cluster of triangle planes using a map of normal vectors, then gripping

Fujita, T. and Aimi, N.
Autonomous Gripping and Carrying of Polyhedral Shaped Object based on Plane Detection by a Quadruped Tracked Mobile Robot.
DOI: 10.5220/0007980905520558
In *Proceedings of the 16th International Conference on Informatics in Control, Automation and Robotics (ICINCO 2019)*, pages 552-558
ISBN: 978-989-758-380-3

was performed by detecting the regions on the surface of the object which can be contacted with the gripper (Harada et al., 2011). Our method is based on similar concept to this approach and is arranged for the grasping by two robotic arms mounted on a mobile robot.

3 OBJECT GRIPPING AND CARRYING

3.1 Overview

In this study, we suppose that a user operates a mobile robot with multiple manipulation arms by remote control in general, finds a target object through images sent from the camera mounted on the robot, then approaches the robot in front of the object. The robot then starts autonomous object gripping and carrying based on plane detection from that circumstance.

The proposed method is as follows. Firstly, the plane information of the object is detected in the environment using a depth sensor. Secondly, sets of two parallel planes that can be reached by the tips of two manipulation arms are extracted so that the solutions of inverse kinematics exist for the both arms. All possible combinations of the set are extracted as candidates of gripping planes. In the inverse kinematics computation, the robot positions as well as the postures of both manipulation arms are also computed. The position of the robot to grip is selected from them such that the movement of the robot from its position at that time becomes minimum. With the gripping position of the robot, then the postures of the manipulation arms are also determined. The robot then moves the position, grips the two planes by two manipulation arms, lifts up the object, and transports it.

This method can be used for a variety of the shape and orientation of object because it is applicable regardless to the number of plane of the object.

3.2 Plane Detection

In this study, we use a depth sensor to detect planes. As a pixel of the depth image can make a 3-D small plane with the next right and under pixels, all small planes are extracted on the depth image. Then, adjacent small planes which have the same normal vector are integrated as one plane. Figure 1 shows an example of the plane integration. The upper panel shows the small planes and their normal vectors extracted from pixels of the depth image and the lower panel shows the integrated planes.

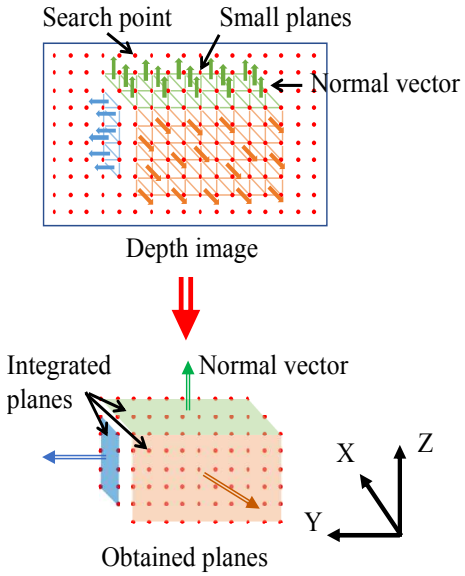

Figure 1: Generation and integration of small planes.

3.3 Gripping Position Detection

Gripping planes for two manipulation arms of the robot are determined from detected planes. To do that, sets of two planes which have the same or opposite directions of normal vector each other are extracted. The sets become candidates for gripping. In this method, horizontal planes to the ground and small planes, which may not be possible to be gripped, are excluded from candidate sets of gripped planes for efficient processing.

The candidate sets are then checked for the possibility of gripping by the left and right manipulation arms using inverse kinematics. Figure 2 shows an overview of this process. Let us assume an environment of flat ground and the robot moves on XY plane for simplicity. The projection line AB on XY plane is extracted by the line connecting two centers of the candidate planes. Let f be the line on XY plane which is orthogonal to the line AB and passing the center point C of AB. We suppose that the robot places on a position R on the line f in the same orientation of the line. Inverse kinematics are computed for each R so that the position of each tip of the left and right manipulators comes each center of the candidate planes in the orientation of the line AB. If solutions of inverse kinematics exist for the both tips, these candidate planes can be gripped by the robot at the position. The set of planes is therefore extracted as a possible set for gripping.

In the extracted all possible sets for gripping, the set in which the movement amount from current position of the robot becomes minimum is determined as the gripping planes.

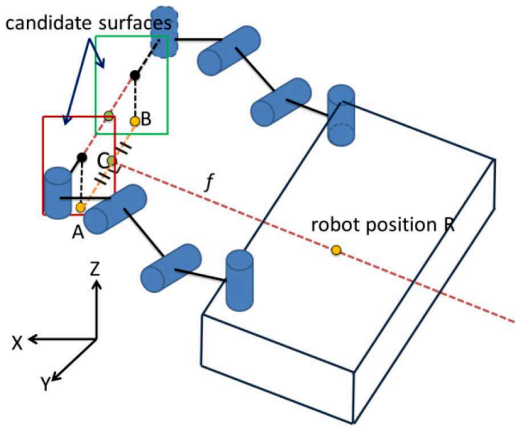

Figure 2: Overview of gripping planes detection.

4 OBSERVATION POSITION DETECTION

4.1 Method

The robot needs to observe the target object from multiple positions to obtain appropriate plane information of the object. To obtain more accurate information, the number of the observation points should be as many as possible. However, when many points are used, it generally takes much time to process. Thus, we try to make decrease the number of observation position as possible; we consider three observation points to obtain valid planes to grip by two manipulation arms.

The robot is in front of the object when starting the autonomous gripping as described in Section 3. Observing the object at the initial position, the robot needs to decide the following observation points which should be in the left and right side. In this study, each position is computed based on the plane information obtained in the initial observation so that whole height of the object is captured and the front plane of the object is captured in the left or right half of the depth image. The computation model is shown in Fig. 3: (a) is a side view and (b) is an upper view to the sensor. We consider the coordinate system depicted in the figure. Detecting the positions of the left and right end points, $\boldsymbol{l}(l_x, l_y)$ and $\boldsymbol{r}(r_x, r_y)$, on XY plane and the top and bottom end points, $\boldsymbol{t}(t_x, t_y)$ and $\boldsymbol{b}(b_x, b_y)$, on XZ plane by the initial observation in front of the object, the height and width of the object become

$$H_o = t_z - b_z \tag{1}$$

and

$$W = l_y - r_y \tag{2}$$

respectively.

Firstly, we determine the distance between the sensor and the object on XZ plane. The minimum distance at which the bottom of the object is captured in the image, D_s, is computed by

$$D_s = H_s \tan\left(\frac{\pi}{2} - \theta_s - \frac{\theta_v}{2}\right) + m \tag{3}$$

where H_s and θ_s are the height and the angle of the mounted sensor, and θ_v is the vertical visual angle of the sensor. The margin m is also given so that the bottom border of the object is captured clearly. In this case, the captured depth at the height of the object, D_t becomes

$$D_t = (H_s - H_o) \tan\left(\frac{\pi}{2} - \theta_s + \frac{\theta_v}{2}\right) \tag{4}$$

where $D_t = \infty$ if $(H_s - H_o) > 0$ and $(\frac{\theta_v}{2} - \theta_s) > 0$ because the top plane of the object is completely captured in the image.

Next, the observation distance on XY plane is computed. As shown in Fig. 3 (b), the sensor faces so that its central axis reaches the left or right end point. Also, the sensor is located so that the opposite end point is fully captured by the sensor image. The minimum distance which meets these conditions is computed by

$$D_h = W \frac{\sin(\theta_h + \varphi)}{\sin\theta_h} \tag{5}$$

where θ_h is the half value of the horizontal visual angle of the sensor, and φ is the angle between the central axis of the sensor and the front plane of the object. As φ is larger, a lot of information for lateral planes can be obtained; on the other side, the error on the front plane may increase and cause some problem in integration of plane information at observation points. We set $\varphi = 135$ degrees in consideration of the trade-off between them.

Then, the distance between the sensor and the object on XY plane, D, has to be larger than D_b and D_h and less than D_t. Therefore, we firstly assume $D = max(D_b, D_h)$. This value is determined as D if $D < D_t$. Otherwise, we set $D = (D_b + D_h)/2$.

Using obtained D, the sensor position on XY plane at the observation point in the right side, $\boldsymbol{C}_\mathrm{r}(C_{rx}, C_{ry})$, is calculated by

$$\boldsymbol{C}_\mathrm{r} = \boldsymbol{r} - D\boldsymbol{p}_\mathrm{r} \tag{6}$$

where $\boldsymbol{p}_\mathrm{r}$ is a unit vector from $\boldsymbol{C}_\mathrm{r}$ to $\boldsymbol{r}$ and obtained by

$$\boldsymbol{p}_\mathrm{r} = \boldsymbol{R}(\varphi - \pi)\boldsymbol{a}_\mathrm{r} \tag{7}$$

where $\boldsymbol{a}_\mathrm{r}$ is a unit vector from $\boldsymbol{r}$ to $\boldsymbol{l}$, and $\boldsymbol{R}(\theta)$ is a rotational matrix for θ angle rotation around Z axis.

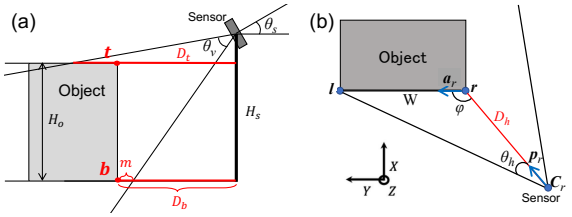

Figure 3: Model for observation position computation (a):side view to the sensor (b):upper view.

In the same way, the sensor position at the observation in the left side, $\boldsymbol{C}_l$, is calculated by

$$\boldsymbol{C}_l = \boldsymbol{l} - D\boldsymbol{p}_\mathrm{l} \tag{8}$$

where $\boldsymbol{p}_\mathrm{l}$ is a unit vector from $\boldsymbol{C}_l$ to $\boldsymbol{l}$ and obtained by

$$\boldsymbol{p}_\mathrm{l} = -\boldsymbol{R}(\pi - \varphi)\boldsymbol{a}_\mathrm{r}. \tag{9}$$

4.2 Computation

We computed the observation points based on the method mentioned above.

Figure 4 shows the experimental settings for the computation. Let us consider the described coordinated system in which the center of the robot at the first observation position O is the origin and forward direction is corresponding to X axis. The object is a lightweight box and has 270 mm, 205 mm, and 150 mm in width, length, and height; thus $H_o = 150$ mm. It is located at (572.5, 0, 0) mm and the robot is located at the first position right in front of the object. The depth sensor is mounted at (170, 0, 163) mm, thus $H_s = 170$ mm, with the tilt angle $\theta_s = 10$ degrees. Its vertical and horizontal visual angles are $\theta_v = 45$ degrees and $\theta_h = 31$ degrees respectively.

In this settings, the second and third observation points, P and Q, which are the right and left sides respectively, were computed. The result is shown in Fig. 5. The margin m was set to 20 mm. Equation (3) led $D_b = 275.9$ mm. Because $(H_s - H_o) > 0$ and $(\frac{\theta_v}{2} - \theta_s) > 0$, $D_t = \infty$ by Equation (4). Equation (5) also gives $D_h = 126.8$ mm. Because of $D_h < D_b$, $D = 275.9$ mm, which resulted the sensor position and robot orientation of $(154.7, -450.3)$ mm and 45 degrees at P, and $(154.7, 450.3)$ mm and -45 degrees at Q. This result shows the valid observation position because the front plane of the object is fully captured in the horizontal visual angle of the sensor.

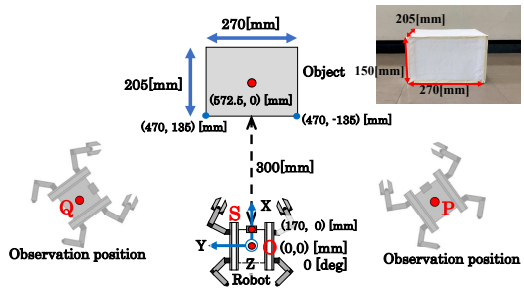

Figure 4: Experimental setup for observation position calculation.

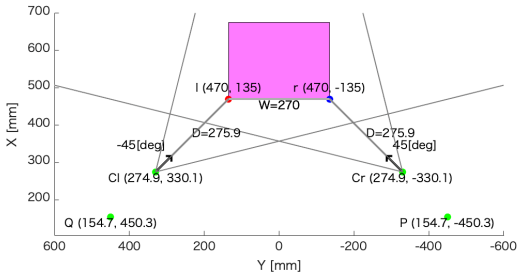

Figure 5: Computed observation positions and angles of view.

5 ROBOT SYSTEM

5.1 Quadruped Tracked Robot

We have implemented these presented methods to quadruped tracked mobile robot which has been developed by the authors (Fujita and Tsuchiya, 2015). Figure 6 shows an overview of the robot. This robot consists of two tracks which drive independently and four 4DOF legs which can be used as manipulation arms. The size of the robot body is 390 mm in length, 420 mm in width, and 170 mm in height. Each of front two legs has a hand unit at the end. The hand unit consists of two curved grippers and can be opened in any angle so that it holds an object having a variety of shape and size; the robot is able to grip an object that has up to 550 mm in width by using two legs.

A depth sensor "Camboard pico flex" by pmd Co. Ltd., the visual angle of which is 60×45 degrees and pixel size is 171×224 pixels, is mounted on the center of the robot body at the height of 163 mm and the 170 mm front from the robot center by tilting 10 degrees. The robot is able to obtain depth information of the area in front of the robot. The computation for detecting object planes, possible gripping positions, and observing points are performed by a host PC LIVA Z (Intel Pentium Processor N4200 1.10 GHz, four

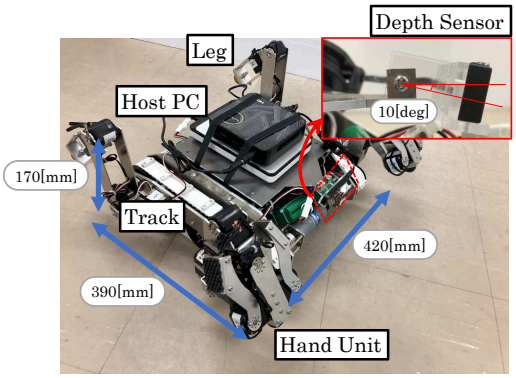

Figure 6: Quadruped tracked mobile robot.

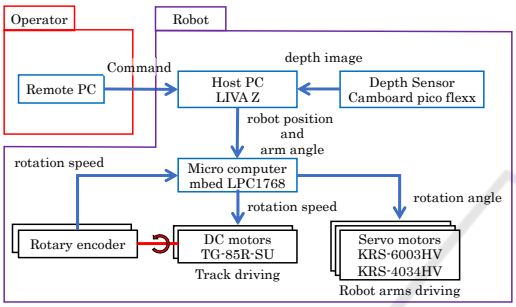

Figure 7: Control system.

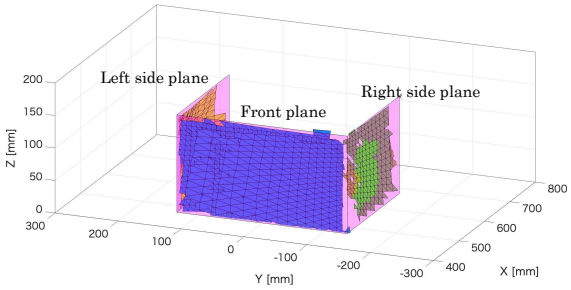

Figure 8: Detected planes of the object.

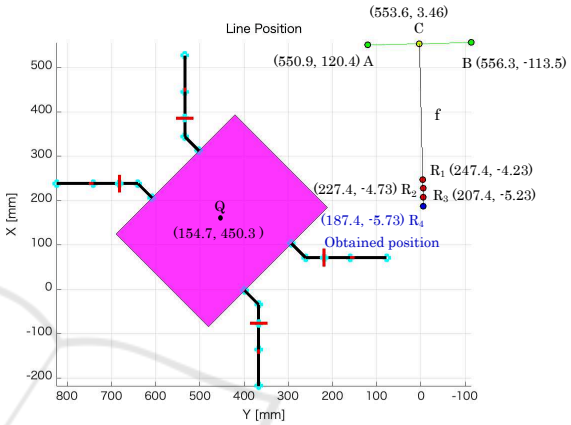

Figure 9: Obtained possible gripping positions.

cores, 16 GB RAM) which is mounted on the top of the robot body.

5.2 Control System

Figure 7 shows the control system for the robot explained above. The track driving and joint angles are controlled by LPC1768, which is an ARM mbed microcomputer.

The host PC on the robot controls the autonomous motion for object gripping and carrying as well as the data processing of the depth sensor and command sending to the microcomputer. An operator sends a motion command to the host PC using the remote PC through wireless network. Because the robot has not mounted a camera yet, the operator moves the robot remotely by watching the robot and object so that it faces right in front the object in this experiment. The robot then starts the autonomous object gripping and carrying based on the presented method.

6 EXPERIMENTS

6.1 Gripping Position Detection

The proposed method for detecting gripping planes and positions was examined. As the first experiment, the robot was placed manually at the observation positions and orientations obtained in the computation described in Section 4.2 in the same setting as shown in Fig. 4. In this experiment, we divided the depth image by 5 pixels interval to make small region, and the planes for the regions were integrated by giving 10 degrees allowance as the angle of identical normal vector. In addition, we assumed the planes that were integrated by 10 or less small planes as noises and eliminated them.

Figure 8 shows a result of detected integrated planes. The blue, green, and yellow planes show detected front, right, and left planes. The magenta planes show the actual planes of the object. This result shows that three planes of the object were detected almost correctly.

Figure 9 shows the result of the detection of possible gripping positions of the robot. Four possible positions, R_1, R_2, R_3, and R_4 were obtained from the detected planes shown in Fig. 8.

Figure 10 shows the result of the gripping position selected from the possible positions. The robot position when they were detected was (154.7, 450.3) mm. Thus, R_4 was selected because it is the shortest distance to move, 457.2 mm, from the position of the robot.

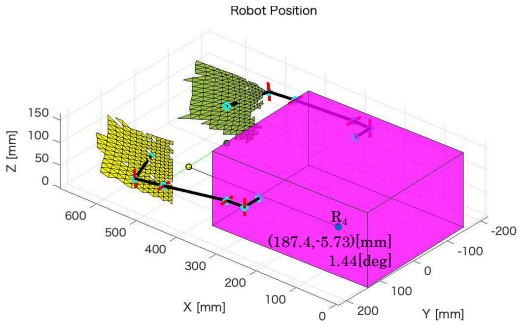

Figure 10: Obtained robot position and arm postures for gripping target object.

Figure 10 also shows the postures of both manipulation arms when gripping the target object. These postures were computed by using inverse-kinematics in detecting possible gripping positions.

These results show that the robot is able to detect valid information for grasping the target object properly.

6.2 Autonomous Gripping and Carrying

We conducted an experiment to examine an autonomous gripping and carrying with the detection of observation points. The experiment was employed on the flat floor in an office room with the same setup to that shown in Fig. 4. The robot was initially at the origin and detected plane information as well as the width and height of the target object at the position. Then the left and right observation points were computed and moved to these positions. The planes detected at three observation points were integrated and possible gripping positions and orientations of the robot with arm postures were computed. The robot finally moved to the gripping position and performed gripping and carrying of the object. Two paths of movement to the observation points were applied: the order of O, P, and Q, or O, Q, and P. Five experiments were performed for each path of movement.

Figure 11 shows a result of computed observation positions. The detected size of the object was 260.1 mm in width and 148.0 mm in height. The magenta area shows actual object position. The computed positions and orientations at the right and left observation points, P and Q, were (160.3, -443.5) mm and 44.9 degrees at P, and (157.9,447.4) mm and -45.1 degrees, respectively. Although these had errors from ideal positions and orientations computed in Section 4.2 for the both positions, the front plane of the object was captured in the view of the sensor to satisfy given condition in computation of the observation points.

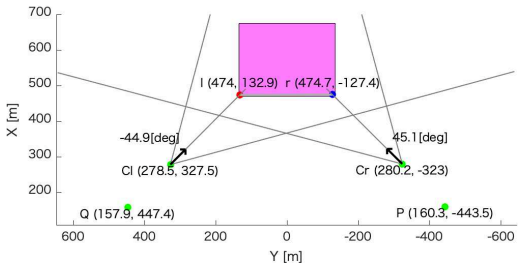

Figure 11: Detected observation positions with angles of view.

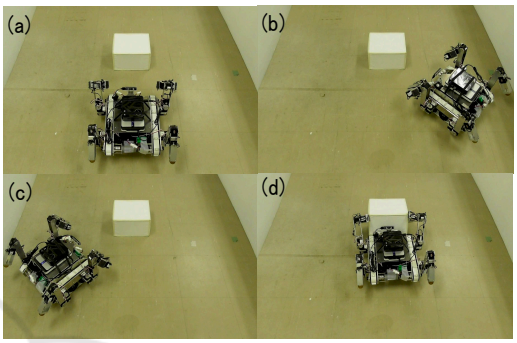

Figure 12: Sequential motion of autonomous gripping and carrying action.

An overview of sequential motion of the robot is shown in Fig. 12. The robot started observation of the target object in front of it in (a), detected its plane information, and obtained next two observation points, P and Q. Then the robot moved to the right observation point P and detected plane information in (b), and the left observation point Q in (c) as well. The plane information detected from three observation points were then integrated and determined the gripping position and orientation of the robot. The robot moved the position and gripped and carried the target object in (d) by moving both arms based on the joint angles computed by inverse kinematics in the detection of possible gripping positions of the robot.

Figure 13 shows position errors of center points on detected planes in the experiment for the movement from the right to the left observation points, from P to Q. The averages and standard deviations of five experiments for this path of movement are indicated. The left two bars show the result in the first experiment described in Section 6.1; the robot was placed manually at the ideal observation positions. The right two bars show the result in this experiment. As the result, this experiment had larger errors than the first experiment, especially for the left plane. We can see that these errors were generated due to localization errors with odometry by actual movement of the robot. The errors in the processes for the detection of plane information must be accumulated as the robot moves.

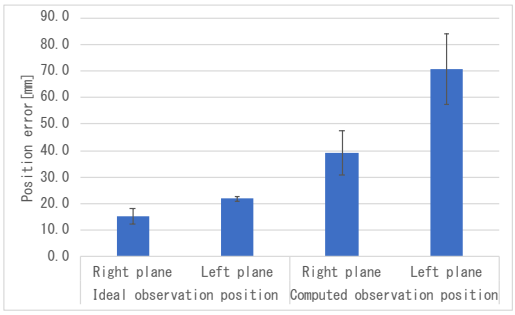

Figure 13: Errors of center positions of detected planes when moving from the right to left observation points.

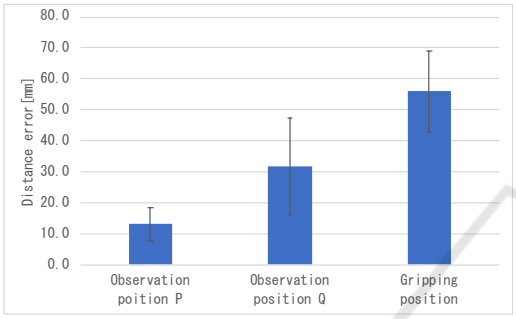

Figure 14: Errors of observation and gripping positions of the robot when moving from the right to left observation points.

In fact, as shown in Fig. 14, the actual position error for the third observation point Q increased to that for the second point P. The same tendency was resulted in the experiment for another path of the movement; the errors for the plane obtained at the third observation point P were larger than that at the second observation point Q.

The error of detected gripping position is also shown in Fig. 14. This was also influenced by the errors of observation positions because it is the last destination after the movement of two observation points. However, we can consider that the error is allowable for the autonomous gripping and carrying by this robot as shown in Fig. 12.

7 CONCLUSIONS

This paper presented a method for autonomous object gripping and carrying for a tracked mobile robot with manipulation arms toward autonomous transportation task in a dangerous site for human. The proposed method enables the robot to obtain gripping position of a polyhedral shaped object based on plane detection. Experimental results showed validity of this method in an environment on the flat floor. As future works, the errors derived from position errors in localization should be decreased. Furthermore, we also need to consider correspondence to robust detection in practical environment with uneven terrain.

REFERENCES

Fujita, T. and Sasaki, T. (2017). Development of Hexapod Tracked Mobile Robot and Its Hybrid Locomotion with Object-Carrying. In *2017 IEEE International Symposium on Robotics and Intelligent Sensors (IRIS2017)*, pages 69–73.

Fujita, T. and Tsuchiya, Y. (2014). Development of a Tracked Mobile Robot Equipped with Two Arms. In *The 40th Annual Conference of the IEEE Industrial Electronics Society (IECON 2014)*, pages 2738–2743.

Fujita, T. and Tsuchiya, Y. (2015). Development of a Quadruped Tracked Mobile Robot. In *The ASME 2015 International Design Engineering Technical Conferences & Computers and Information in Engineering Conference IDETC/CIE*.

Gu, S., Su, M., Zhu, H., Guan, Y., Rojas, J., and Zhang, H. (2017). Efficient pole detection and grasping for autonomous biped climbing robots. In *2017 IEEE International Conference on Robotics and Biomimetics (ROBIO)*, pages 246–251.

Gu, S., Zhu, H., Li, H., Guan, Y., and Zhang, H. (2018). Optimal collision-free grip planning for biped climbing robots in complex truss environment. *Applied Sciences*, 8(12).

Harada, K., Tsuji, T., Nagata, K., Yamanobe, N., Maruyama, K., Nakamura, A., and Kawai, Y. (2011). Grasp planning for parallel grippers with flexibility on its grasping surface. In *Proceedings of IEEE International Conference on Robotics and Biomimetics*, pages 1540–1546.

Masuda, H. and Lim, H.-o. (2014). Retinal model based plane detection method using range images for unknown object recognition (in japanese). *Journal of the Robotics Society of Japan*, 32(1):64–73.

Yamazaki, K., Tomono, M., and Tsubouchi, T. (2007). Picking up and unknown object through autonmous modeling and grasping by a mobile manipulator. In *Proceedings of the 6th International Conference on Field and Service Robotics*, pages 563–571.